Supporting Information

Multifunctional Metal–Organic Framework as A Versatile Nanoplatform for Aβ Oligomer Imaging and Chemo-Photothermal Treatment in Living Cells

Xueyan Yan[1, ‡], Yixin Pan[2, ‡], Liang Ji[1], Jinyu Gu[1], Yuanyuan Hu[1], Yi Xia[1], Chenglin Li[1], Xinguang Zhou[3,], Dongzhi Yang[1], Yanyan Yu[1,*]*

[1] Jiangsu Key Laboratory of New Drug Research and Clinical Pharmacy, Xuzhou Medical University, 209 Tongshan Road, Xuzhou 221004, Jiangsu, P.R.China

[2] Department of Neurosurgery, Center for Functional Neurosurgery, Ruijin Hospital, affiliated with Shanghai Jiao Tong University School of Medicine, Ruijin Hospital, 197 RuijinEr Road, Shanghai 200025, P. R. China

[3] Shenzhen NTEK Testing Technology Co., Ltd., Shenzhen 518000, Guangdong, P. R. China

Email address: yyyxzmc@163.com; Aaron@ntek.org.cn

‡ These authors contributed equally to this work.

1. Experimental

1.1 Instruments

1.2 Synthesis of CeONP

1.3 Synthesis of CeONP@ZIF-8

1.4 Cell culture and assessment of cell viability

1.5 Flow cytometry analysis

1.6 ABTS free radical scavenging and SOD, catalase activity assays

1.7 ROS detection in SH-SY5Y cells

1.8 JC-1 staining

1.9 TUNEL analysis

1.10 Calcein AM/PI staining

2. Results and Discussion

2.1 TEM images of ZIF-8/PDA and CeONP NPs (Figure S1)

2.2 DLS measurements of ZIF-8, ZIF-8/PDA, CeONP@ZIF-8 and CeONP-Res-PCM@ZIF-8/PDA (Figure S2)

2.3 SEM images of ZIF-8, ZIF-8/PDA, CeONP@ZIF-8 and CeONP-Res-PCM@ZIF-8/PDA (Figure S3)

2.4 Zeta potential of ZIF-8, ZIF-8/PDA, CeONP@ZIF-8 and CeONP-Res-PCM@ZIF-8/PDA (Figure S4)

2.5 The pore size distribution profile of ZIF-8, ZIF-8/PDA, CeONP@ZIF-8 and CeONP-Res-PCM@ZIF-8/PDA (Figure S5)

2.6 Stability of CeONP-Res-PCM@ZIF-8/PDA/Apt nanocomposite in H_2O, Tris-HCl and cell culture (Figure S6)

2.7 Optimizations (Figure S7)

2.8 Biostability investigation on the probe (Figure S8)

2.9 The cytotoxicity of different nanocomposite on SH-SY5Y and BV-2 cells (Figure S9)

2.10 Flow cytometry quantitative analysis of CeONP-Res-PCM@ZIF-8/PDA/Apt in SH-SY5Y cells (Figure S10)

2.11 Confocal images of CeONP-Res-PCM@ZIF-8/PDA/Apt nanocomposite in SH-SY5Y cells with different incubation time (Figure S11)

2.12 Standard curve of different concentration Res (Figure S12)

2.13 ROS scavenging ability of CeONP@ZIF-8/PDA (Figure S13)

2.14 Confocal images and flow cytometry analysis of ThT and DCFH-DA fluorescence intensities of SH-SY5Y cells under different treatments (Figure S14)

2.15 Calcium-AM/PI staining of live/dead cells and flow cytometry analysis of the mitochondrial membrane potential in SH-SY5Y cells (Figure S15)

2.16 Comparison of our work with other detection assays for Aβ (Table S1)

3. References

1. Experimental

1.1 Instruments

The hydrodynamic diameters and Zeta potentials were determined using a Malvern Zeta Sizer Nano-ZS instrument. Scanning electron microscope images (SEM) were taken on scanning electron microscopy (Teneo, ThermoFisher Scientific). Elemental mappings were performed on a field emission gun Hitachi S-4800 scanning electron microscope operating at 1 kV (Hitachi Co. Ltd., Tokyo, Japan). Transmission electron microscopy images (TEM) were recorded with a FEI-TECNAI G2 transmission electron microscope operating at 200 kV. X-ray photoelectron spectroscopy (XPS) measurements were taken on an ESCA Lab MKII X-ray photoelectron spectrometer using Mg Kα radiation. The crystal structure of samples was determined by X-ray diffractometer (XRD) (Bruker D8 Advance). N_2 adsorption-desorption measurements were performed on a micromeritics instrument (ASAP2020). Fluorescence spectra were recorded by Fluorescence spectrophotometer (Agllent Biosciences Co., Ltd, USA). CCK-8 assay was performed using Varioskan Flash microplate reader (ThermoFisher Scientific) at 450 nm. Fluorescence images were recorded using IX73 (Olympus, Japan) with iXon X3885 EMCCD (Andor, England). Flow cytometry was carried out using NovoCyte flow cytometer (Agillent Biosciences Co., Ltd, USA).

1.2 Synthesis of CeONP

Firstly, CeONP was synthesized in aqueous solution using reported method.[1] A solution containing 1.0 M cerium (III) nitrate was slowly added to 30.0 mL ammonium hydroxide under continuous stirring for 2 h, during which, the color of the solution changed from deep brown to light yellow, indicating the formation of CeONP. The obtained product was washed with distilled water and centrifuged at 4,000 rpm for several times, until the pH of supernatant became neutral. Finally, the CeONP was resuspended in distilled water.

1.3 Synthesis of CeONP@ZIF-8

3.5 mg of CeONP nanopolyhedra and 100 mg of PVP were dissolved with 5 mL methanol solution, stirred at room temperature for 24 h, collected by centrifugation, and stored in 100 μL of methanol to obtain PVP-CeONP. Then, 3.5 mg of PVP-CeONP was added into 0.9 mL aqueous solution of 3.15 mM 2-MIM, followed by addition and

incubation with 0.1 mL of 0.045 mM zinc acetate dehydrate at room temperature for 5 min. The products were centrifuged at 12,000 rpm for 10 min and washed with methanol for three times. At last, the CeONP@ZIF-8 nanomaterials were obtained by vacuum drying.

1.4 Cell Culture and Assessment of Cell Viability

SH-SY5Y and BV-2 cells were cultured in DMEM medium with 10% FBS, penicillin (100 units/mL) and streptomycin (100 μg/mL). One day before imaging, the cells were placed on glass-bottomed dishes (SPL), which were incubated in a humidified atmosphere containing 5% (v/v) CO_2 at 37°C.

In vitro cytotoxicity of CeONP-Res-PCM@ZIF-8/PDA/Apt was assessed using a standard CCK-8 assay. The SH-SY5Y and BV-2 cells were seeded in 96-well plates (5×10^4/well) and grown at 37°C overnight, after which, different concentrations of CeONP-Res-PCM@ZIF-8/PDA/Apt (20, 40, 60, 80 μg/mL) were added and incubated for 48 h. After that, the medium was replaced by addition of 10 μL CCK-8 reagent to each well and incubated for another 2 h. Finally, Bio-Rad 680 microplate reader at 450 nm was used to measure the absorbance of each well.

1.5 Flow Cytometry Analysis

SH-SY5Y cells were cultured in 6-well plates (3×10^5 / well) for 24 h, and then incubated with 1mL $A\beta_{1\text{-}40}$ (30 μM) overnight. Res, CeONP, ZIF-8/PDA and CeONP-Res-PCM@ZIF-8/PDA/Apt (-/+NIR) (60 μg/mL) was incubated with cells at 37°C for 48 h. After resuspended, cells were stained with corresponding fluorescent dyes and then rinsed for three times in PBS. Finally, the assay was performed by flow cytometer.

1.6 ABTS Free Radical Scavenging and SOD, Catalase Activity Assays

ABTS scavenging assay was used to evaluate the antioxidant activity of CeONP, ZIF-8, ZIF-8/PDA, CeONP@ZIF-8 and CeONP@ZIF-8/PDA. Firstly, the ABTS free radical ($ABTS^{\bullet+}$) was generated through the reaction of ABTS stock solution (5 mM, dissolved in PBS) and manganese bioxide according to the previously described method.[2] Then, CeONP, ZIF-8, ZIF-8/PDA, CeONP@ZIF-8 and CeONP@ZIF-8/PDA (60 μg/mL) were respectively mixed with $ABTS^{\bullet+}$ radical solution, and the absorbance at 734 nm within 60 min was measured by a UV-*vis* spectrophotometer.

The superoxide scavenging activity was assessed using a SOD Assay Kit-WST

(Sigma-Aldrich). Firstly, CeONP, ZIF-8, ZIF-8/PDA, CeONP@ZIF-8 and CeONP@ZIF-8/PDA (60 μg/mL) were respectively mixed with 200 μL WST-8 working solution. The SOD coupling reaction was initiated by addition of 20 μL xanthine oxidase solution and incubated at 37°C for 20 min. The absorbance at 450 nm, which was proportional to SOD activity, was measured using a microplate reader. An amount of 50 U/mL SOD was defined as the activity of the enzyme that inhibited the reduction reaction of WST-8 with superoxide anion by 50% in experiments quantifying SOD-mimetic activity. Three repeated sets of measurements were performed.

The hydrogen peroxide scavenging activity was evaluated by Titanium Sulfate Colorimetry assay. Firstly, 0.3 g titanium sulfate was added to 6mL distilled water to form a 5% titanium sulfate solution and stored at 4°C. Then, 1 mL of 3.2 mM H_2O_2 was mixed with CeONP, ZIF-8, ZIF-8/PDA, CeONP@ZIF-8 and CeONP@ZIF-8/PDA (60 μg/mL) respectively, followed by addition of 0.2 mL alkaline base fluid and 5% titanium sulfate to each tube. After mixing well, the solutions were placed for 5 min at room temperature and centrifuged at 12,000 g for 15 min, discarding the supernatant. 2 mL acidic base solution was added to the sediment of each tube and shacked to completely dissolve the sediment. The absorbance of each solution at 412 nm was measured by a UV-*vis* spectrophotometer.

1.7 ROS Detection in SH-SY5Y Cells

SH-SY5Y cells were firstly cultured in 6-well plates (3×10^5/well) for 24 h, and then incubated with 1 mL $A\beta_{1-40}$ (30 μM) overnight. Then, the cells were incubated with 60 μg/mL Res, CeONP, ZIF-8/PDA and CeONP-Res-PCM@ZIF-8/PDA (-/+NIR) for 48 h, respectively. SH-SY5Y cells without Aβ and materials were served as controls. Cells were then treated with 10 μM DCFHDA for 30 min, and the intracellular ROS levels in these cells were monitored under CLSM.

1.8 JC-1 Staining

Mitochondria were stained with the JC-1 staining kit following the protocol of manufacturer. SH-SY5Y cells containing $A\beta_{1-40}$ (30 μM) were incubated with Res, CeONP, ZIF-8/PDA and CeONP-Res-PCM@ZIF-8/PDA (-/+NIR) (60 μg/mL) for 24 h, respectively. SH-SY5Y cells without Aβ and materials were served as controls. The culture medium was replaced, and cells were washed twice using staining buffer. 1 mL

JC-1 staining solution was then added, and cells were incubated at 37°C for 20 min. Meanwhile, the nuclei were stained with DAPI, followed by washing the samples with PBS and fluorescent images were taken under a fluorescence microscope under CLSM.

1.9 TUNEL Analysis

SH-SY5Y cells containing $A\beta_{1-40}$ (30 μM) were incubated overnight. Then, Res, CeONP, ZIF-8/PDA and CeONP-Res-PCM@ZIF-8/PDA/Apt (60 μg/mL) were separately added to the medium, and CeONP-Res-PCM@ZIF-8/PDA/Apt were subjected to NIR treatment for 5 min. After co-cultivation for 48 h, the cells were fixed with 4.0% paraformaldehyde. Subsequently, SH-SY5Y cells were cultured with TUNEL solution for 1 h in the dark. Sample were rinsed thoroughly with PBS. Then the nuclei was stained with DAPI, followed by washing with PBS. Finally, SH-SY5Y cells were observed under CLSM.

1.10 Calcein AM/PI Staining

SH-SY5Y cells containing $A\beta_{1-40}$ (30 μM) were incubated overnight. Then, Res, CeONP, ZIF-8/PDA and CeONP-Res-PCM@ZIF-8/PDA/Apt (60 μg/mL) were separately added to the medium and received NIR treatment for 5 min for CeONP-Res-PCM@ZIF-8/PDA/Apt group. After co-cultivation for 48 h, the culture medium was removed and washed with PBS. The cells were then stained with 500 μL Calcein AM/PI for 5 min and rinsed. Finally, the green and red fluorescence were observed under fluorescence microscopy.

2. Results and Discussion

2.1 TEM images of ZIF-8/PDA and CeONP NPs

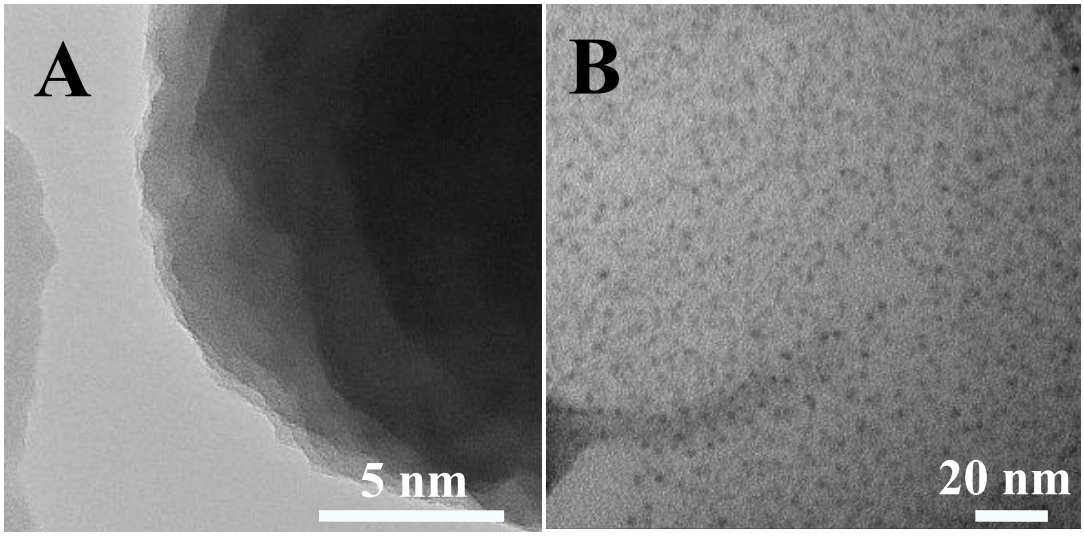

Figure S1. TEM images of ZIF-8/PDA (A) and CeONP NPs (B).

2.2 DLS measurements of ZIF-8, ZIF-8/PDA, CeONP@ZIF-8 and CeONP-Res-PCM@ZIF-8/PDA

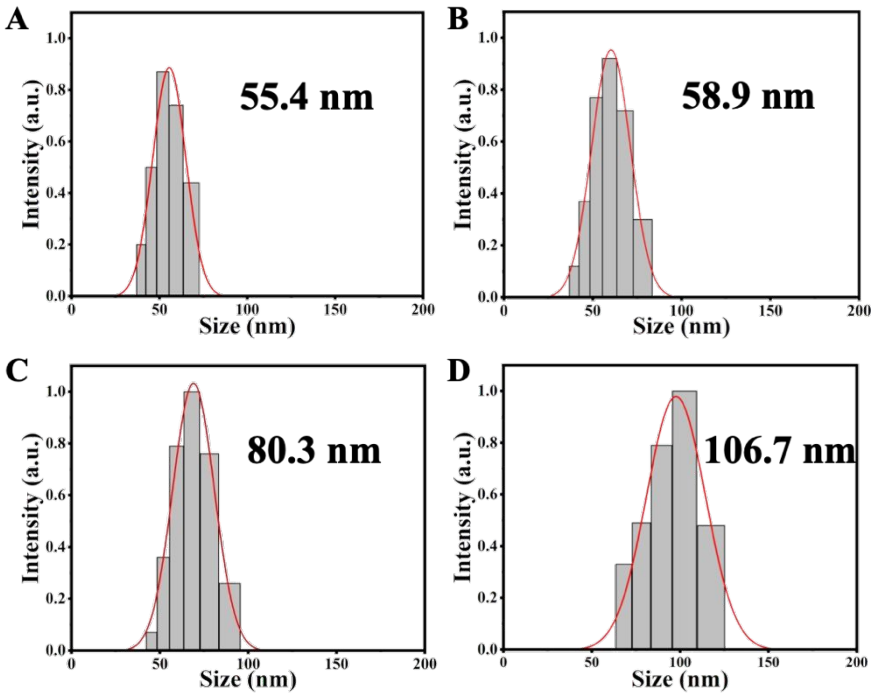

Figure S2. Size distributions of ZIF-8 (A), ZIF-8/PDA (B), CeONP@ZIF-8 (C) and CeONP-Res-PCM@ZIF-8/PDA (D).

2.3 SEM images of ZIF-8, ZIF-8/PDA, CeONP@ZIF-8 and CeONP-Res-PCM@ZIF-8/PDA

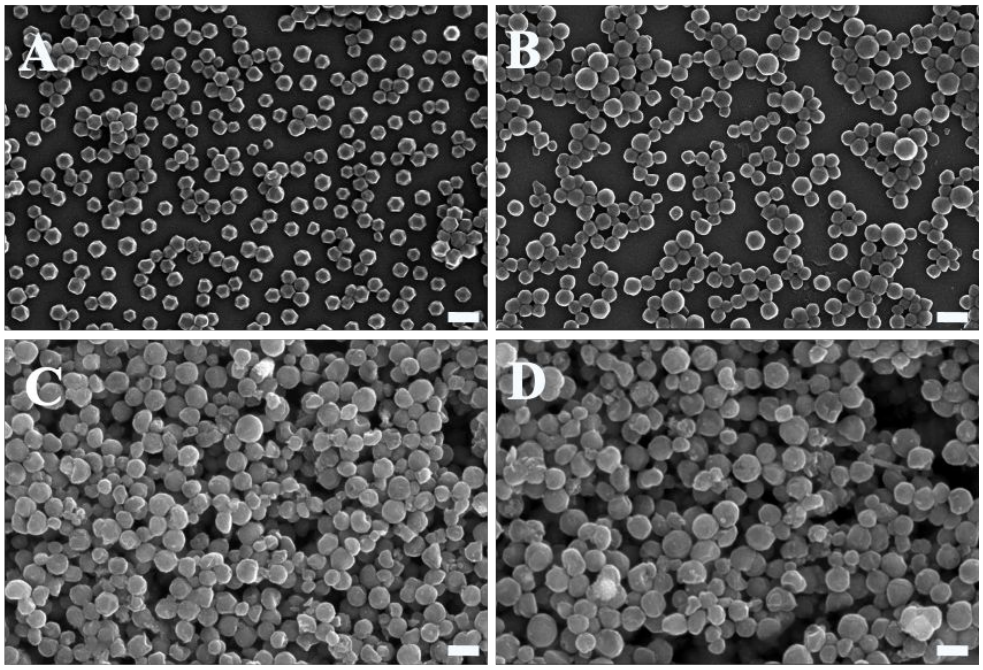

Figure S3. SEM images of ZIF-8 (A), ZIF-8/PDA (B), CeONP@ZIF-8 (C) and CeONP-Res-PCM@ZIF-8/PDA (D). Scale bars represented 100 nm.

2.4 Zeta potential of ZIF-8, ZIF-8/PDA, CeONP@ZIF-8 and CeONP-Res-PCM@ZIF-8/PDA

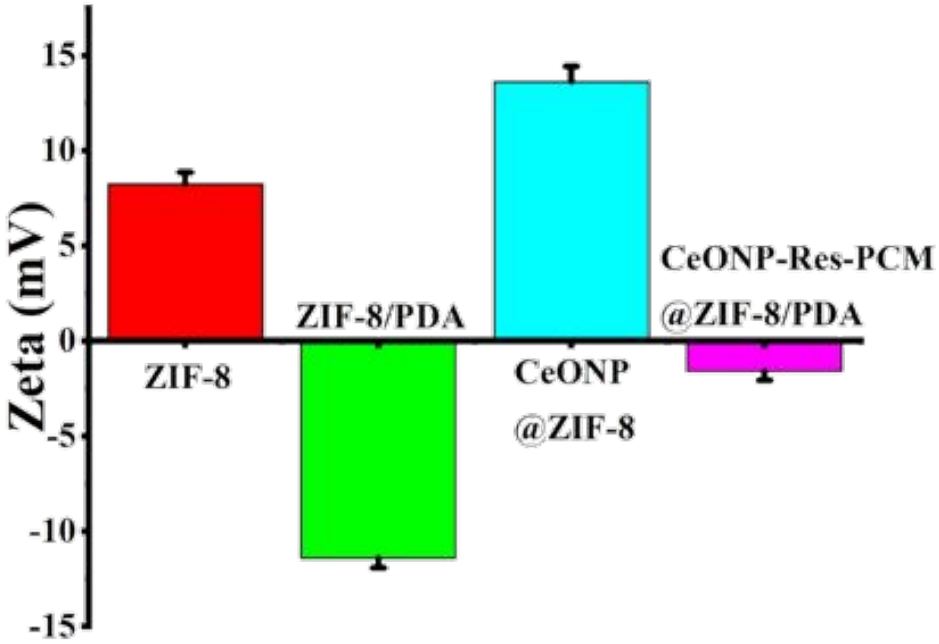

Figure S4. Zeta potential of ZIF-8, ZIF-8/PDA, CeONP@ZIF-8 and CeONP-Res-PCM@ZIF-8/PDA.

2.5 The pore size distribution profile of ZIF-8, ZIF-8/PDA, CeONP@ZIF-8 and CeONP- Res-PCM@ZIF-8/PDA

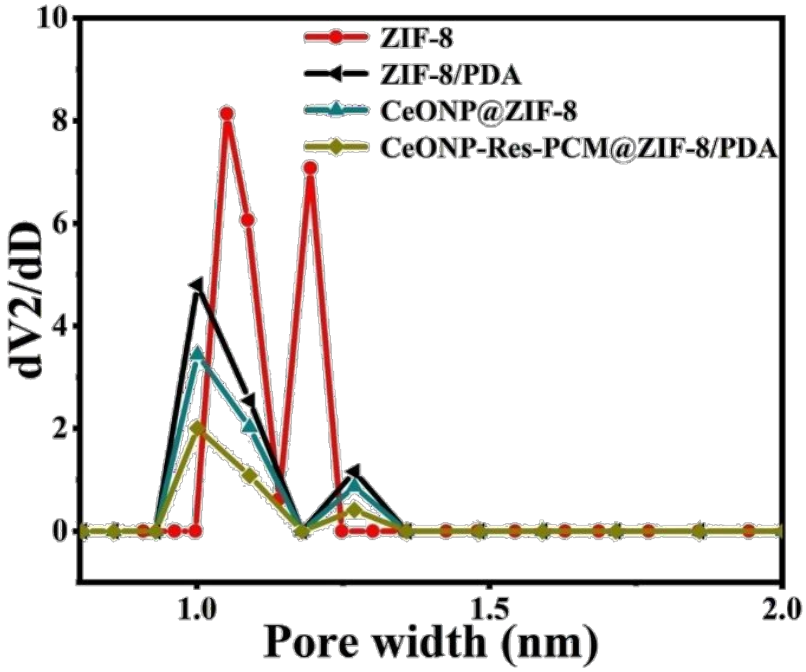

Figure S5. The pore size distribution profile of ZIF-8, ZIF-8/PDA, CeONP@ZIF-8 and CeONP-Res-PCM@ZIF-8/PDA.

2.6 Stability of CeONP-Res-PCM@ZIF-8/PDA/Apt nanocomposite in H_2O, Tris-HCl (pH 7.4) and cell culture

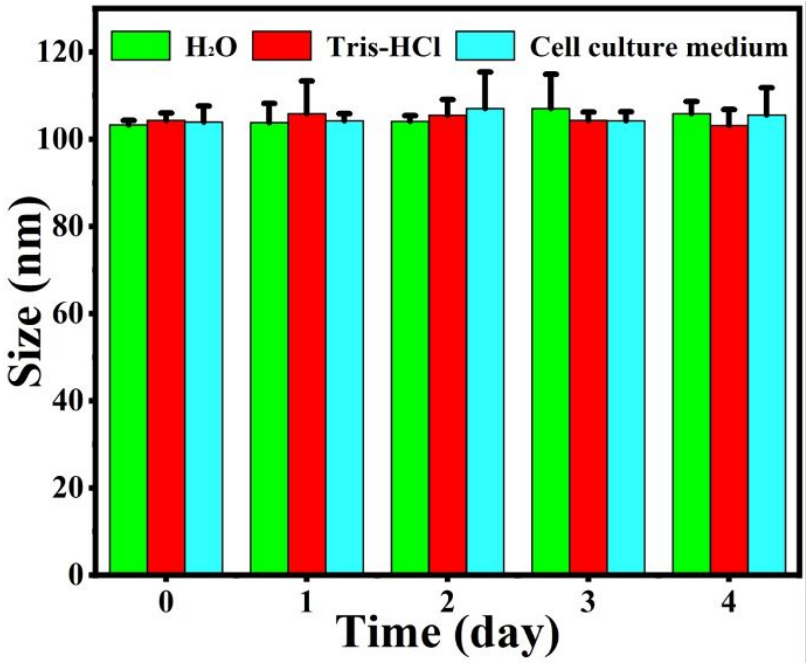

Figure S6. Stability of CeONP-Res-PCM@ZIF-8/PDA/Apt nanocomposite in H_2O, Tris-HCl (pH 7.4) and cell culture.

2.7 Optimizations

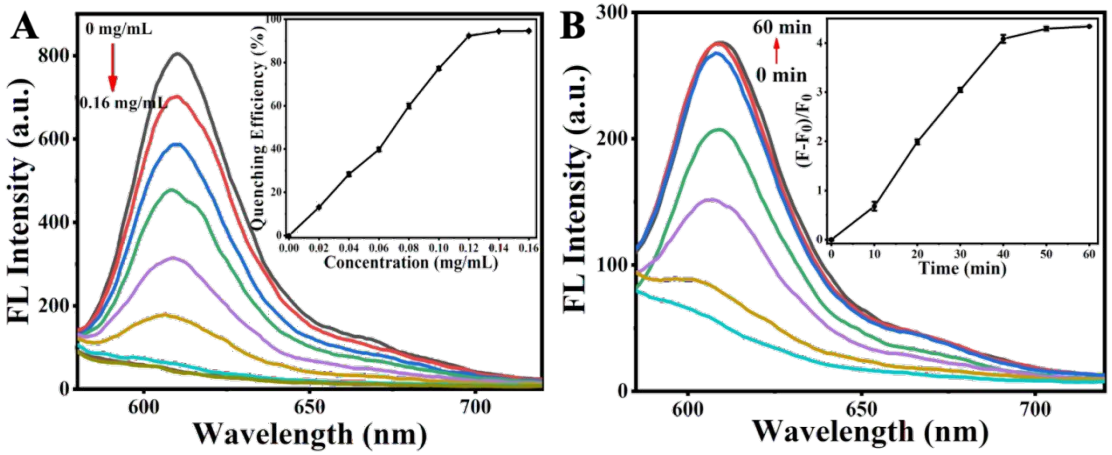

Figure S7. (A) Fluorescence spectra and tendency curve (inset) of 50 nM Texas-red-Apt in the presence of CeONP-Res-PCM@ZIF-8/PDA with a series of concentrations (0, 0.02, 0.04, 0.06, 0.08, 0.10, 0.12, 0.14, 0.16 mg/mL). (B) Dependence of fluorescence intensity on incubation time toward 50 μM AβO.

2.8 Biostability investigation on the probe

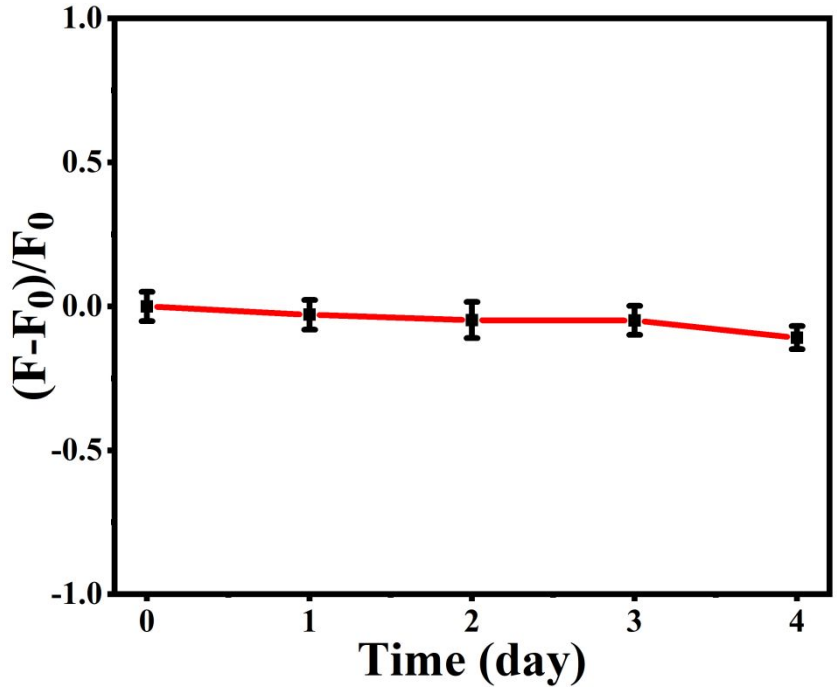

Figure S8. The fluorescence responses of the CeONP-Res-PCM@ZIF-8/PDA/Apt probe toward 10 μM AβO obtained on different storage time.

2.9 The cytotoxicity of different nanocomposite on SH-SY5Y and BV-2 cells

In order to verify whether the designed CeONP-Res-PCM@ZIF-8/PDA/Apt nanocomposite could be used in biological application, intracellular AβO imaging was determined. Firstly, CCK-8 assays were performed to evaluate the cytotoxicity of CeONP, Res, ZIF-8/PDA and CeONP-Res-PCM@ZIF-8/PDA/Apt with or without NIR (**Figure S8**). As observed, after incubated cells with different concentrations of materials for 48 h, both of SH-SY5Y and BV-2 cells maintained high cell viability (basically over 90%), which indicated that the nanoprobe had little cytotoxicity or side effects on living cells and was biocompatible enough to be further applied into intracellular detection and imaging.

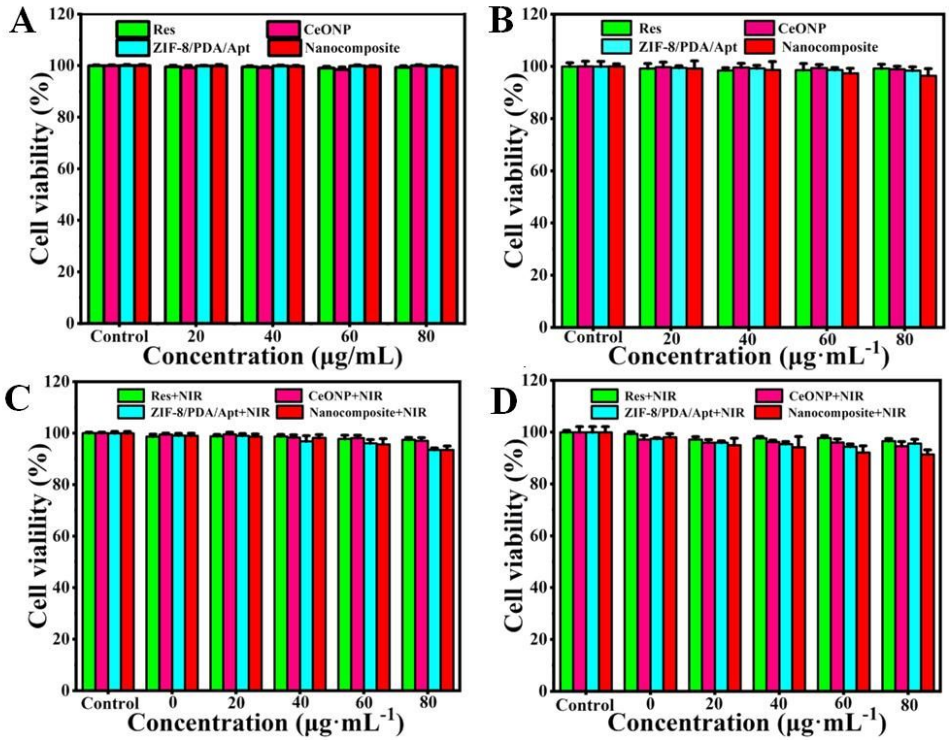

Figure S9. The effects of Res, CeONP, ZIF-8/PDA/Apt, and CeONP-Res-PCM@ZIF-8/PDA/Apt nanocomposite on the viability of SH-SY5Y (A, C) and BV-2 (B, D) cells incubated for 48 h with or without NIR irradiation.

2.10 Flow cytometry quantitative analysis of CeONP-Res-PCM@ZIF-8/PDA/Apt in SH-SY5Y cells

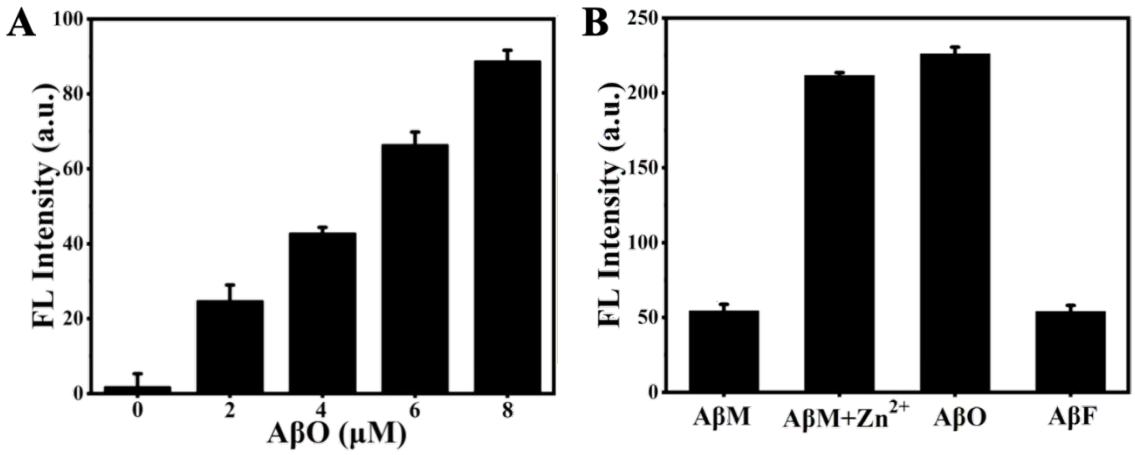

Figure S10. Flow cytometry analysis of CeONP-Res-PCM@ZIF-8/PDA/Apt in SH-SY5Y cells treated with different concentrations of AβO (A) and AβM, AβM + Zn^{2+}, AβO and AβF (B).

2.11 Confocal images of CeONP-Res-PCM@ZIF-8/PDA/Apt nanocomposite in SH-SY5Y cells with different incubation time

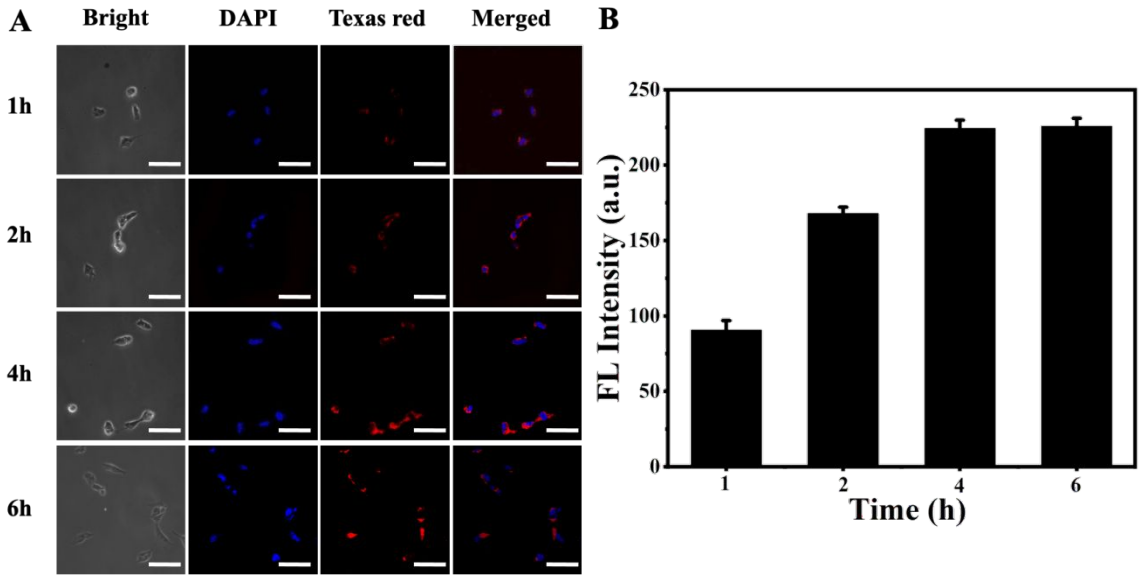

Figure S11. (A) Confocal images of nanocomposite in SH-SY5Y cells with different incubation time. Scale bars represented 30 μm. (B) Quantitative analysis of fluorescence intensity determined by flow cytometry.

2.12 Standard curve of different concentration resveratrol

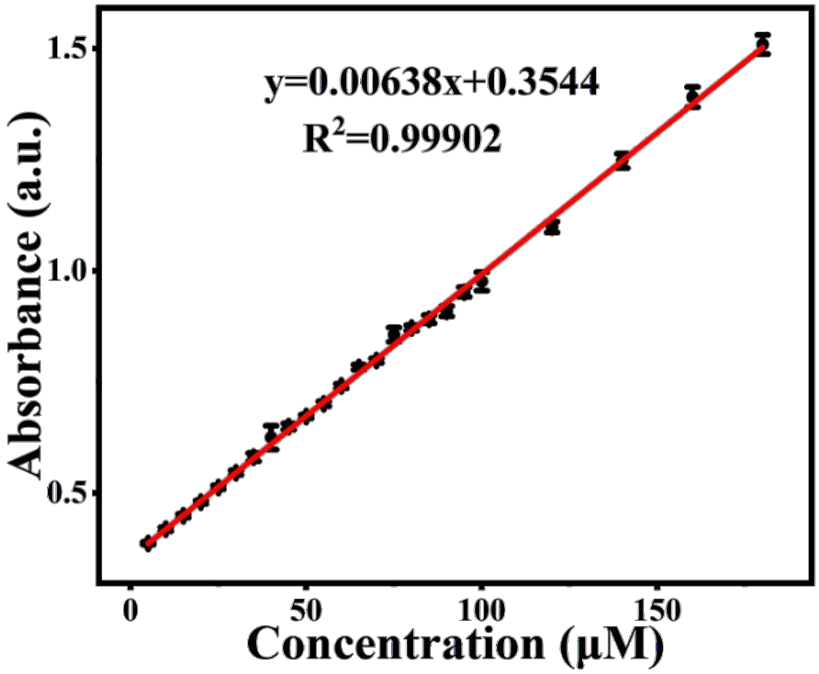

Figure S12. Standard curve of different concentration resveratrol.

2.13 ROS scavenging ability of CeONP@ZIF-8/PDA

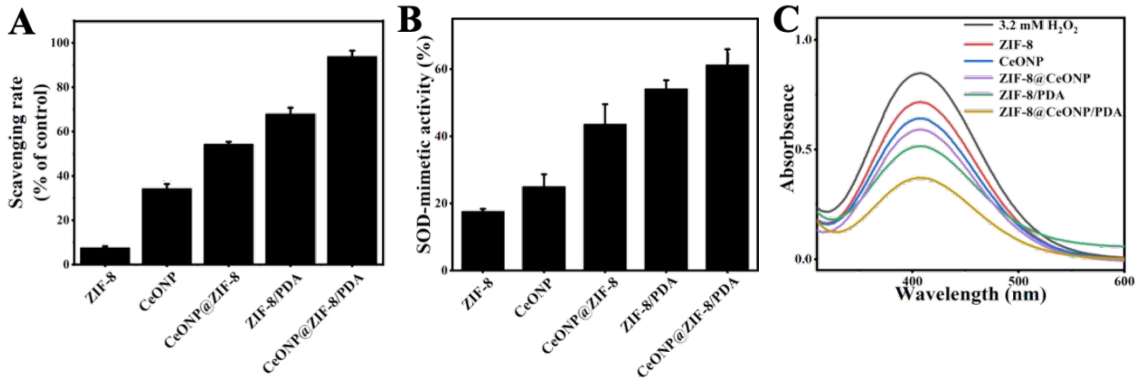

Figure S13. (A) *In vitro* antioxidant activities of ZIF-8, CeONP, CeONP@ZIF-8, ZIF-8/PDA and CeONP@ZIF-8/PDA. (B) SOD-mimetic abilities of ZIF-8, CeONP, CeONP@ZIF-8, ZIF-8/PDA and CeONP@ZIF-8/PDA. (C) UV-*vis* spectra of 3.2 mM H_2O_2 solution treated with different materials.

2.14 Confocal images and flow cytometry analysis of ThT and DCFH-DA fluorescence intensities of SH-SY5Y cells under different treatments

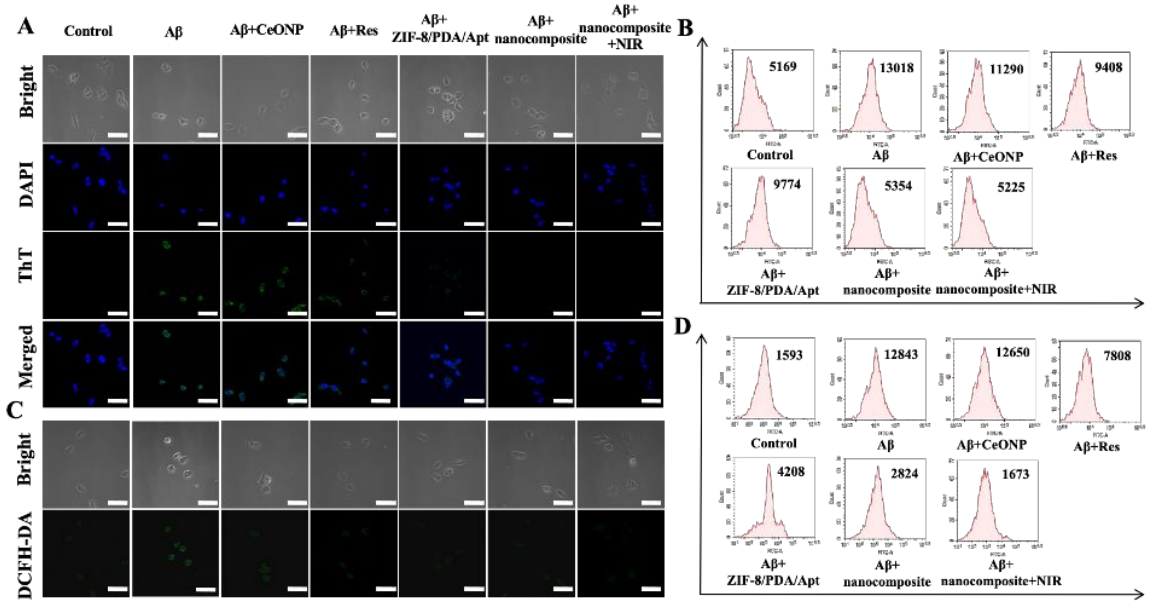

Figure S14. (A) Confocal microscopy images and (B) flow cytometry analysis of ThT fluorescence intensities of SH-SY5Y cells treated with CeONP, Res, ZIF-8/PDA/Apt and the nanocomposite with or without NIR irradiation in the presence of Aβ. (C) Confocal fluorescence images and (D) DCFH-DA fluorescence intensities of intracellular ROS in SH-SY5Y cells treated with CeONP, Res, ZIF-8/PDA/Apt and the nanocomposite with or without NIR irradiation in the presence of Aβ. Scale bars represented 30 μm.

2.15 Calcium-AM/PI staining of live/dead cells and flow cytometry analysis of the mitochondrial membrane potential in SH-SY5Y cells

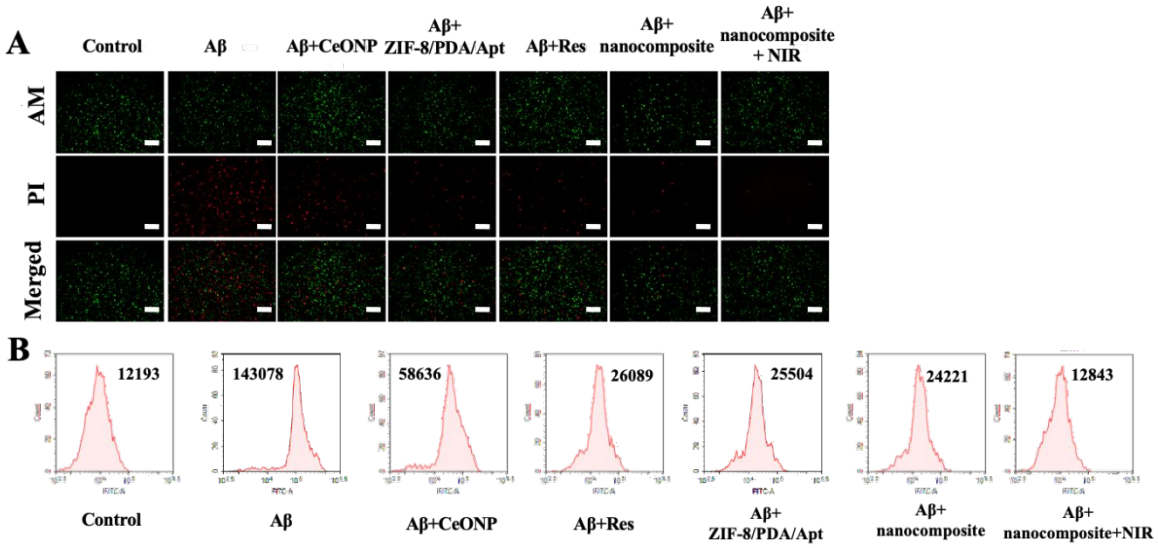

Figure S15. (A) Calcium-AM/PI staining of SH-SY5Y cells under different treatments. Scale bars represented 25 μm. (B) Flow cytometry analysis of the mitochondrial membrane potential depletion under different treatments.

2.16 Comparison of our work with other detection assays for Aβ

Table S1. Comparison of our work with other detection assays for Aβ

	Probe	Sensing	Detection sensitivity	Applications	Reference
Inorganic nanomaterials	CuO/g-C_3N4	Photoelectro-chemical	5.79 fM	/	[2]
	PDANS	Fluorescence	12.5 nM	/	[3]
	ZIF-8-ferrocene	UV-*vis*	500 nM	/	[4]
	MSe-Res/Fc-β-CD/Bor	/	/	CT treatment	[5]
	MoS_2/AuNRs	/	/	CT/PTT treatment	[6]
	Au-POM	Fluorescence	/	PTT/CT treatment	[7]
	rPOMs@MSNs@copolymer	/		PTT treatment	[8]
Organic molecules	Quinoline-based AIE probe	Fluorescence	26.9 nM	Imaging in AD rat brain sections	[9]
	BoDipy-Oligomer	Fluorescence	/	AβO staining in live AD brain	[10]
	Quinoline-malononitrile-based NIR probe	Fluorescence	1-10 μM	Imaging in AD rat brain sections	[11]
	Hybrid structure of naphthalene and quinoxaline	Fluorescence	/	Discrimination of Aβ and Tau aggregates	[12]
ZIF-8 based probe	CeONP-Res-PCM@ZIF-8/PDA/Apt	Fluorescence	3.2 nM	CT/PTT treatment	This work

3. References

(1) Guan, Y.; Li, M.; Dong, K.; Gao, N.; Ren, J.; Zheng, Y.; Qu, X., Ceria/POMs hybrid nanoparticles as a mimicking metallopeptidase for treatment of neurotoxicity of amyloid-β peptide. *Biomaterials* **2016,** *98*, 92-102.

(2) Zhang, J. L., Zhang, X. C., Gao, Y., Yan, J. Y., Song, W. B. Integrating CuO/g-C_3N_4 p-n heterojunctioned photocathode with MoS_2 QDs@Cu NWs multifunctional signal amplifier for ultrasensitive detection of AβO. *Biosens Bioelectron*. **2021**, *176*, 112945-112954.

(3) Liu, L., Chang, Y., Yu, J., Jiang, M. S., Xia, N. Two-in-one polydopamine nanospheres for fluorescent determination of beta-amyloid oligomers and inhibition of beta-amyloid aggregation. *Sensor Actuat B-Chem*. **2017**, *251*, 359-365.

(4) Qin, J. L., Cho, M., Lee, Y. Ferrocene-Encapsulated Zn Zeolitic Imidazole Framework (ZIF-8) for Optical and Electrochemical Sensing of Amyloid-beta Oligomers and for the Early Diagnosis of Alzheimer's Disease. *ACS Appl Mater Interfaces*. **2019**,

11(12), 11743-11748.

(5) Sun, J., Wei, C. F., Liu, Y. N., Xie, W. J., Xu, M. M., Zhou, H., Liu, J. Progressive release of mesoporous nano-selenium delivery system for the multi-channel synergistic treatment of Alzheimer's disease. *Biomaterials*. **2019**, *197*, 417-431.

(6) Wang, X. H., Han, Q. S., Liu, X. L., Wang, C., Yang, R. Multifunctional inhibitors of beta-amyloid aggregation based on MoS_2/AuNR nanocomposites with high near-infrared absorption. *Nanoscale*. **2019**, *11(18)*, 9185-9193.

(7) Meng, L., Guan, Y., Zhao, A., Ren, J. S., Qu, X. G. Using Multifunctional Peptide Conjugated Au Nanorods for Monitoring beta-amyloid Aggregation and Chemo-Photothermal Treatment of Alzheimer's Disease. *Theranostics*. **2017**, *7(12)*, 2996-3006.

(8) Ma, M. M., Nan, G., Sun, Y. H., Du, X. B., Ren, J. S., Qu, X. G. Redox-Activated Near-Infrared-Responsive Polyoxometalates Used for Photothermal Treatment of Alzheimer's Disease. *Adv Healthc Mater*. **2018**, *7(20)*, 1800320-1800327.

(9) Wang, Y. X., Qiu, Y. T., Sun, A. Y., Xiong, Y. H., Tan, H. Y., Shi, Y. Q., Yu, P., Roy, G., Zhang, L., Yan, J. Dual-functional AIE fluorescent probes for imaging β-amyloid plaques and lipid droplets. *Anal Chimi Acta*. **2020**, *1133*, 109-118.

(10) Teoh, C. L., Su, D. D., Sahu, S., Yun, S. W., Drummond, E., Prelli, F., Lim, S., Cho, S., Ham, S., Wisniewski, T., Chang, Y. T. Chemical Fluorescent Probe for Detection of Aβ Oligomers. *J. Am. Chem. Soc*. **2015**, *137*, 13503−13509.

(11) Xu, M. Y., Li, R. H., Li, X., Lv, G. L., Li, S. P., Sun, A. Y., Zhou, Y. F., Yi, T. NIR fluorescence probes with good water-solubility for detection of amyloid beta aggregates in Alzheimer's disease. *J. Mater. Chem. B*. **2019**, *7 (36)*, 5535-5540.

(12) Zhou, K. X., Yuan, C., Dai, B., Wang, K., Chen, Y. M., Ma, D. L., Dai, J. P., Liang, Y, Tan, H. W., Cui, M. C. Environment-Sensitive Near-Infrared Probe for Fluorescent Discrimination of A β and Tau Fibrils in AD Brain. *J. Med. Chem*. **2019**, *62*, 6694-6704.